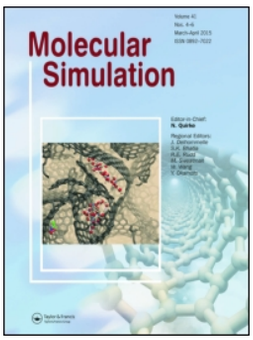

Molecular Simulation

ISSN: 0892-7022 (Print) 1029-0435 (Online) Journal homepage: https://www.tandfonline.com/loi/gmos20

Self-assembly of polymer-like structures of magnetic colloids: Langevin dynamics study of basic topologies

D. A. Rozhkov, E. S. Pyanzina, E. V. Novak, J. J. Cerdà, T. Sintes, M. Ronti, P. A. Sánchez & S. S. Kantorovich

To cite this article: D. A. Rozhkov, E. S. Pyanzina, E. V. Novak, J. J. Cerdà, T. Sintes, M. Ronti, P. A. Sánchez & S. S. Kantorovich (2018) Self-assembly of polymer-like structures of magnetic colloids: Langevin dynamics study of basic topologies, Molecular Simulation, 44:6, 507-515, DOI: 10.1080/08927022.2017.1378815

To link to this article: https://doi.org/10.1080/08927022.2017.1378815

Published online: 28 Sep 2017.

MOLECULAR SIMULATION, 2018
VOL. 44, NO. 6, 507–515
https://doi.org/10.1080/08927022.2017.1378815

Taylor & Francis
Taylor & Francis Group

Self-assembly of polymer-like structures of magnetic colloids: Langevin dynamics study of basic topologies

D. A. Rozhkov[a,c], E. S. Pyanzina[a], E. V. Novak[a], J. J. Cerdà[b], T. Sintes[b], M. Ronti[c], P. A. Sánchez[c] and S. S. Kantorovich[a,c]

[a]Institute of Natural Sciences and Mathematics, Ural Federal University, Ekaterinburg, Russia; [b]Physics Department, University of the Balearic Islands, Palma de Mallorca, Spain; [c]Computational Physics, University of Vienna, Vienna, Austria

ABSTRACT

We study the self-assembly of colloidal magnetic particles permanently cross-linked into polymer-like structures with different topologies, that we call supracolloidal magnetic polymers (SMPs). In order to understand the influence of the interparticle permanent links, we investigate SMPs holding the main topologies observed in the self-assembly of non-cross-linked magnetic particles via grand canonical Monte Carlo simulations: chains, rings and simple branched structures. Here, using molecular dynamics simulations, we focus on systems of SMP pairs. Our results evidence that the presence of crosslinkers leads to the formation of new types of aggregates, not previously observed for individual magnetic colloids.

ARTICLE HISTORY
Received 29 July 2017
Accepted 4 September 2017

KEYWORDS
Magnetic colloidal particles; self-assembly; cross-linked polymer-like structures; Langevin dynamics simulations

1. Introduction

The fundamental understanding of the self-assembly properties of colloidal systems is one of the key topics in current research on novel microstructured soft materials and technologies. Available experimental techniques allow the synthesis of colloidal particles with sizes ranging from the micrometre to the nanometre scale from a wide variety of substances and with a high control on their chemical and physical properties. This places colloidal particles among the most versatile building blocks in bottom-up strategies for the design of advanced materials, including cutting-edge approaches such as that ones based on hierarchical self-assembly [1,2].

Colloids with defined self-assembly properties are particularly useful for the design of stimuli-responsive soft materials, i.e. soft matter systems that experience a controlled change in their properties as a response to some particular external drive [3]. One of the most important cases is the combination of magnetic colloidal particles with carrier substances, like liquids and/or polymers, in order to create materials responsive to external magnetic fields. Whereas many substances common in soft matter systems are significantly sensitive to other stimuli such as temperature, pH, electric fields or chemical reagents, their magnetic properties are practically negligible under most conditions of interest for technological applications. The introduction of micro or nanoparticles of magnetic substances – typically, solid metallic compounds – is therefore, essential for the creation of magnetoresponsive soft materials. The fact that only the magnetic particles within such systems are sensitive to the external stimulus represents an advantage for many practical applications, providing a high control on the response of the material [4,5].

Magnetic colloidal particles and materials based on them have been intensively studied for already several decades and keep attracting a growing research interest, mainly stimulated by their unique properties and the development of the experimental techniques for the synthesis of colloidal hybrid materials. The simplest and most extensively studied magnetoresponsive soft materials are ferrofluids and magnetorheological fluids, which are dispersions of magnetic colloidal particles in a liquid carrier fluid [6–9]. These materials show strong changes in their rheological properties under the influence of external magnetic fields and/or cooling. Such macroscopic changes emerge as a consequence of the spontaneous self-assembly or field-induced assembly of the magnetic particles into chain-like structures – typically, linear chains, rings and branched chains – driven by the strongly anisotropic nature of their magnetic interactions [10–14]. This characteristic self-assembly behaviour of magnetic colloidal particles is also determinant for the properties of more complex soft magnetic materials, including polymer hybrid materials such as magnetic gels and elastomers [15–17].

The aforementioned soft magnetic materials – conventional magnetic fluids, gels and elastomers – are usually obtained by means of relatively simple experimental techniques – basically, the dispersion or a large amount of magnetic colloidal particles in a liquid carrier and/or the filling of a polymer matrix with them. This provides a limited control on the detailed microstructure of such systems. A much more sophisticated approach is the creation of small aggregates of magnetic particles with a well-defined structure that can be later used as building blocks of more complex systems, following the bottom-up approach to materials synthesis. The most straightforward structures for such small building blocks are the aforementioned self-assembled chains of magnetic colloidal particles. In particular, linear polymer-like chains are relatively easy to obtain under external fields. These systems were initially studied as micromechanical sensors [18], microfluidic artificial cilia,

CONTACT S. S. Kantorovich sofia.kantorovich@univie.ac.at

propellers and pumpers [19–22] and contrast agents in magnetic resonance imaging diagnostics [23]. They also have been proposed for other applications, like magnetically tunable photonic crystals [24], or as building blocks of more complex structures such as polymer brush-like magnetoresponsive coatings [25–28]. In some of such examples, the magnetic chains can keep their linear structure with the sole help of the magnetic interactions between the particles. However, in many cases it is convenient to permanently stabilise the chain-like structures by cross-linking the neighbouring particles with polymers. This provides a much higher resistance to mechanical stresses, a significantly increased magnetic response [29] and a total independence from the self-assembly conditions of the particles after the cross-linking, with the only potential downside of obtaining a much higher rigidity of the chains. The latter property, however, can be tuned by selecting the composition and length of the polymer crosslinkers [30,31]. Even this tuning has been achieved to date only for microparticles, cutting-edge experimental techniques like DNA designed self-assembly [32,33] or in situ polymer mineralisation [34,35] open up the possibility to also create rather flexible linear polymer-like chains of magnetic nanoparticles. Such techniques also may allow the permanent stabilisation of small polymer-like aggregates with morphologies more complex than the simple linear chain. From now on, we will use the generic term 'supracolloidal magnetic polymers' (SMPs) to name these systems.

The detailed characterisation of the equilibrium structures of SMPs has started to be thoroughly explored very recently. The rich structural behaviour predicted even for single linear chains [36–38] and their polymer brush-like arrangements [26–28] points these materials as promising building blocks of sophisticated self-assembled supracolloidal systems with strong magnetic response. Inspired by the possibility of the experimental achievement of more complex morphologies for these stabilised chain-like aggregates, here we extend our preliminary work on the self-assembly properties of pairs of linear chains and rings of cross-linked ferromagnetic colloids [39] to the rest of the most basic structures, observed experimentally in dispersions of free magnetic particles and characterised by simple models of conventional ferrofluids, like the system of dipolar hard spheres [14]. Based on this latter system, very recently we presented a grand canonical Monte Carlo simulation study aimed at understanding the properties of single clusters of ferromagnetic colloids [40]. In this study, we could estimate the probabilities of finding a cluster of a given size and/or topology depending on temperature. Our simulations confirmed the importance of the competition between four basic morphologies: chain, ring, three-point branched structure – or 'Y'-junction – and the four-point branched structure – or 'X'-junction [40]. We also discovered that to observe branching or ring formation even at relatively low temperature, the cluster should contain not less than seven to eight dipolar hard spheres. Examples of these self-assembled clusters of 20 dipolar spheres are provided in Figure 1. Based on these findings, we decided to study SMPs of several lengths, to allow for the variations in the configurational entropy.

The idea to permanently cross-link the four basic self-assembled structures observed for magnetic collidal particles in dispersion is based on the assumption that such clusters formed by spontaneous or simple field-induced self-assembly might be experimentally easier to stabilise with polymer cross-linking techniques. In order to study the self-assembly properties of such prospective supracolloidal building blocks, here we perform extensive computer simulations using a bead-spring model of SMPs for every one of the four basic morphologies: linear chain, ring, X-junction and Y-junction. We focus on the equilibrium structures driven by the magnetic interactions of pairs of identical small aggregates in absence of external fields, analysing the dependence of their self-assembly behaviour on their morphology, size and magnetic strength.

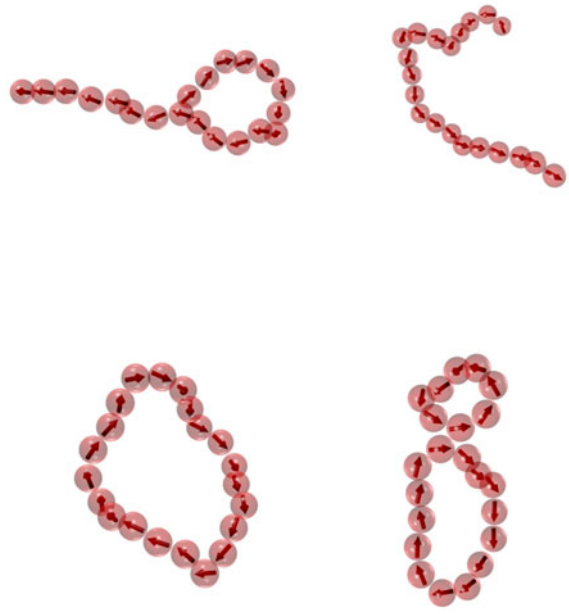

Figure 1. (Colour online) Examples of the four basic different topologies of aggregates obtained in grand canonical Monte Carlo simulations for dipolar hard spheres. In these examples all the self-assembled structures have size $L = 20$.

The work is organised as follows. First, we introduce our bead-spring model of SMPs and the details of the simulation approach. Then, the simulation results obtained for the equilibrium structures of two SMPs of given topology are presented and analysed, discussing the different self-assembled structures observed depending on the interaction range between the two stabilised aggregates. Finally, the summary of the work can be found in the last Section.

2. Methods

2.1. A model of stabilised polymer-like aggregates of magnetic colloids

We assume the magnetic colloids in our system to be identical spherical solid bodies of a ferromagnetic material, composed of a single magnetic domain, that are coated with a thin layer of soft polymer material in order to individually stabilise them in the carrier fluid and to allow their cross-linking. Under this assumption, the magnetic properties of the colloids can be represented by a permanent point magnetic dipole, $\vec{\mu}$, fixed at the centre of the sphere. Therefore, any pair of magnetic particles i and j, carrying magnetic moments $\vec{\mu}_i$ and $\vec{\mu}_j$, respectively,

interact by means of the conventional dipole–dipole potential,

$$U_{dd}(\vec{r}_{ij};\vec{\mu}_i,\vec{\mu}_j) = \frac{\vec{\mu}_i\cdot\vec{\mu}_j}{r^3} - \frac{3\left[\vec{\mu}_i\cdot\vec{r}_{ij}\right]\left[\vec{\mu}_j\cdot\vec{r}_{ij}\right]}{r^5}, \quad (1)$$

where $r = \left\|\vec{r}_{ij}\right\| = \left\|\vec{r}_i - \vec{r}_j\right\|$ is the displacement vector between the centres of the particles. For the modelling of the non-magnetic interactions in our system of SMPs, we choose a coarse-grained approach based on a bead-spring representation, as is frequent in simulations of polymer–magnetic colloidal particle composites [41–46]. Specifically, the magnetic colloids are modelled as soft spheres of characteristic diameter σ, interacting with a Weeks-Chandler-Andersen (WCA) pair potential [47]

$$U_{\mathrm{WCA}}(r;\epsilon_s,\sigma,r_{\mathrm{cut}}) = \begin{cases} U_{\mathrm{LJ}}(r;\epsilon_s,\sigma) - U_{\mathrm{LJ}}(r_{\mathrm{cut}};\epsilon_s,\sigma), & r < r_{\mathrm{cut}} \\ 0, & r \geq r_{\mathrm{cut}} \end{cases}, \quad (2)$$

where $U_{\mathrm{LJ}}(r)$ is the conventional Lennard–Jones (LJ) potential with the potential well depth ϵ_s, $U_{\mathrm{LJ}}(r;\epsilon_s,\sigma) = 4\epsilon_s[(\sigma/r)^{12} - (\sigma/r)^6]$, that in expression (2) is truncated at the position of its minimum, $r_{\mathrm{cut}} = 2^{1/6}\sigma$, and shifted by its corresponding depth, $U_{\mathrm{LJ}}(r_{cut})$, to make the interaction purely repulsive. Finally, the effects of the polymer crosslinkers that stabilise the aggregates of magnetic particles into polymer-like chain structures are modelled by means of a particular spring-like bonding potential that takes into account the mechanical constrains introduced by the crosslinkers on both, the centre-to-centre distance between the bonded particles and the relative orientations of their dipole moments. This potential includes two terms, defined by the following expression:

$$U_S(\vec{r}_{ij},\hat{\mu}_i,\hat{\mu}_j) = \frac{K_S}{2}\left[\left(\vec{r}_{ij} - (\hat{\mu}_i+\hat{\mu}_j)\frac{\sigma}{2}\right)^2 - r_{\mathrm{max}}^2\ \ln\left(1 - \left[\frac{\vec{r}_{ij}}{r_{\mathrm{max}}}\right]^2\right)\right], \quad (3)$$

where K_S is the general prefactor that determines the energy scale of the interaction, $\hat{\mu}_i = \vec{\mu}_i/\left\|\vec{\mu}_i\right\|$ and $\hat{\mu}_j = \vec{\mu}_j/\left\|\vec{\mu}_j\right\|$ are the unitary vectors parallel to each dipole moment and r_{max} is the maximum allowed centre-to-centre distance. The first term in such expression, introduced in our preliminary works [29,36], is mainly intended to penalise the misalignment of the dipoles from their head-to-tail arrangement. It is basically equivalent to link the particles with a harmonic spring of elastic constant K_S whose ends are attached to points on the particles surfaces – i.e. to points at distance $\sigma/2$ from their centres – corresponding to the projection of the head of one of the dipoles and the tail of the other one, respectively. Therefore, the first term in expression (3) defines a maximum of two bonding points for each particle, but does not limit the number of neighbours linked to them. Figure 2(a) shows a sketch of this part of the bonding scheme, in which the magnetic particles are represented as spherical beads, with a central arrow indicating the orientation of their dipoles, and the bonds as springs. The sketched example represents a minimal Y-junction, in which the central particle has one bonding point connected to one neighbour whereas the other bonding point is linked to two neighbours. The second term of

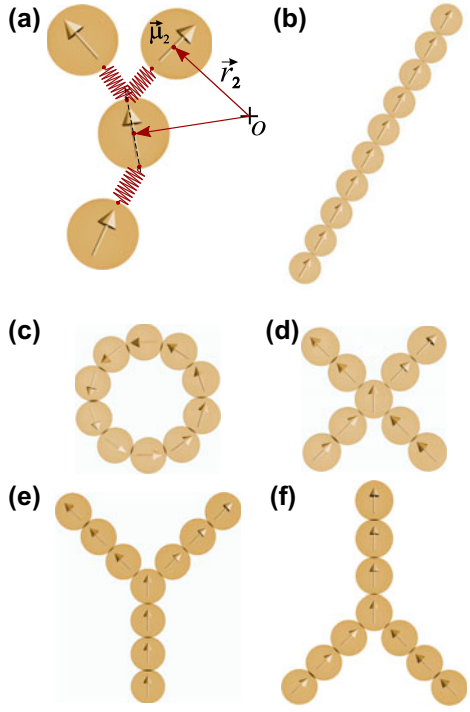

Figure 2. (Colour online) (a) Bead-spring model for the cross-linking of magnetic colloids forming polymer-like stabilised aggregates. See the main text for details. (b–f) Examples of the five different topologies of aggregates simulated in this work, all with size $L = 10$ except (d): (b) linear chain; (c) ring; (d) X-junction of size $L = 9$; (e) Type 1 Y-junction; (f) Type 2 Y-junction.

the bonding potential corresponds to an isotropic attraction, defined as the standard finitely extensible non-linear elastic (FENE) bonding potential. As pointed above, the FENE term simply prevents the bonding distance to go beyond r_{max}. This term is important to avoid unrealistic arrangements of particles from different aggregates due to the unlimited extensibility of the bond allowed by the first term.

The modelling approach described above allows to easily represent any of the basic branched and non-branched chain morphologies to be studied here. Such morphologies are sketched in Figures 2(b) to 2(f), in this case without showing the bonding springs. The depicted examples correspond to the minimal sizes – measured as the amount of particles in the aggregate, L – explored in this work for every given morphology. For symmetry reasons, non-branched structures – linear chains and rings – and four-point branched ones – X-junctions – are uniquely defined by their backbone shape. Three-point branched structures, instead, allow to define two different morphologies with the same shape, as shown in Figures 2(e) and (f), that correspond to different orientations of the dipoles at the branching points. We named the case in which the central particle is bonded to one dipole head and two dipole tails as type 1 Y-junction (Y1), whereas the case of bonding to two dipole heads and one tail is named type 2 Y-junction (Y2). The simulation approach employed to study the self-assembly behaviour of these five different morphologies is described in the next Section.

2.2. Simulation details

With the model introduced above, we performed molecular dynamics simulations in the canonical ensemble. No periodic

boundary conditions were applied. We used a Langevin thermostat in order to approximate implicitly the effects of the thermal fluctuations of the background fluid on the magnetic beads [48,49]. This means that the movements of each bead i are governed by the translational and rotational Langevin equations, obtained by adding an stochastic and a friction terms to the Newtonian equations of motion:

$$m_i(\mathrm{d}\vec{v}_i/\mathrm{d}t) = \vec{F}_i - \Gamma_\mathrm{T}\vec{v}_i + \vec{\xi}_{i,\mathrm{T}}, \quad (4)$$

$$\vec{I}_i \cdot (\mathrm{d}\vec{\omega}_i/\mathrm{d}t) = \vec{\tau}_i - \Gamma_\mathrm{R}\vec{\omega}_i + \vec{\xi}_{i,\mathrm{R}}, \quad (5)$$

where $\vec{F}_i$ and $\vec{\tau}_i$ are the total force and torque acting on the particle, m_i is the particle mass and $\vec{I}_i$ its inertia tensor. Finally, Γ_T and Γ_R are the translational and rotational friction constants, and $\vec{\xi}_{i,\mathrm{T}}$ and $\vec{\xi}_{i,\mathrm{R}}$ a Gaussian random force and torque, respectively, fulfilling the normal fluctuation–dissipation rules.

In this work, we used unitary inertia tensors in order to ensure isotropic rotations in the system. Since here we are only interested in the equilibrium behaviour and not in the system dynamics, the friction terms in Equations (4) and (5) can be chosen arbitrarily. We chose $\Gamma_\mathrm{T} = 1$ and $\Gamma_\mathrm{R} = 3/4$ as values known for providing a fast relaxation in this type of simulations [50,51].

Our coarse-grained modelling approach makes convenient the use of reduced units. System energies are measured in the scale of the soft core repulsions, $\epsilon_s = 1$. In all the simulations, we used a reduced system temperature $T = 1$, defined as the ratio between the actual thermal energy and the chosen energy scale. Distances and masses are measured in units defined by the characteristic diameter of the beads, $\sigma = 1$, and their mass, $m = 1$. Finally, grounded on our previous studies on linear chain structures [29,36], we chose $K_S = 30$ and $r_\mathrm{max} = 1.5$ for the bonding interactions.

The systems we simulated here consist of two identical aggregates with a given size, L, and squared moment of the dipoles, μ^2, in a simulation box with open boundaries. The aggregates are placed symmetrically in the simulation box at a minimum separation distance d between them, with an initial configuration corresponding to perfectly ideal arrangements of each shape. In order to control their relative separation during the simulation, the central particle of each aggregate is permanently fixed in its initial placement, forbidding its displacements but not its rotations. This central particle is the middle one in linear chains, the particle at the branching position in X, Y1 and Y2 shapes, and an arbitrary one in rings. The choice to fix these very particles was made because of the branched structures, in which the middle particle corresponded to the branching point, i.e. to the particle which, in comparison to other particles in the SMP, was less likely to form an extra bond. The simulation protocol consisted of an initial warm-up of the initial configurations at $T = 4$, performing 10^5 integration steps with a time step $\delta t = 5 \cdot 10^{-5}$. After the warm-up, the systems were equilibrated at $T = 1$ for $9 \cdot 10^5$ integration steps, using a time step $\delta t = 5 \cdot 10^{-3}$. Finally, a production cycle of $3 \cdot 10^6$ steps was performed, in which the system configurations were measured at intervals of 10^5 steps. With this protocol we studied the effects of different morphologies, sizes and dipole moments of the aggregates on the self-assembly behaviour of identical pairs as a function of their relative distance. By considering only two SMPs and fixing the distance between them, we make an idealised approximation to the conditions corresponding to different concentrations of monodisperse SMPs solutions. We sampled all the morphologies introduced above, using sizes $L = 9$ and $L = 25$ for the X-junction shape and $L = 10$ and $L = 25$ for the rest, three different values for the dipole moments, $\mu^2 = \{3, 5, 8\}$, and relative separation distances within the interval $d/L \in [0.1,\ 1.1]$. The small size of the systems under study allowed us to avoid the use of any approximate method for the calculation of the long-range magnetic interactions that were computed by simple direct sum. The simulations were carried out with the package ESPResSo 3.3.1 [52,53].

3. Results and discussion

We start the discussion by analysing the probability of two identical SMPs, being in equilibrium at a relative separation d/L, to form an amount C of energy driven close contact connections between their magnetic particles. This simple parameter will help us to identify the different self-assembled structures that may appear. In order to compute C, we first define the centre-to-centre separation threshold for two particles to be considered in close contact as $r_{ij} \leq 1.2$. Since the only attractive interaction in the system corresponds to favourable arrangements of the magnetic dipoles, we also impose the condition of the dipole–dipole pair energy of the involved particles, given by Equation (1), to be non-positive, $U_{dd}(\vec{r}_{ij}) \leq 0$. Finally, in this calculation we do not distinguish the connections formed between pairs of particles belonging to the same or to different SMPs, but we exclude any pair corresponding to permanently bonded particles. Thus, C gives us a quantitative indication of the self-assembly in the systems.

Figure 3 shows the probability distributions of two linear SMPs to form C energy driven connections, as a function of their relative separation d/L, for several selected values of dipole moment and SMP size. Several typical configurations for $L = 10$ are also provided inside the plots. One can see that for $\mu^2 = 3$, independently from L and the distance between the central particles, the two SMPs are not forming any energy driven connections with significant probability. Only for $d/L = 0.1$, the central particles, fixed next to each other, reorient their dipole moments in such a way that their interaction is favourable. From this observation, one can expect a very weak self-assembly in dispersions of linear SMPs with $\mu^2 = 3$, even in a broad range of concentrations. The same conclusion holds also for SMPs with size $L = 25$, however, their distributions tend to be slightly more irregular due to their larger configurational entropy. This weak dependence on the size of the SMPs within the sampled range of parameters has been also observed for the rest of systems under study. Thus, without loss of qualitative generality, from now on we will discuss only the behaviour of systems with shortest SMPs. As is expected, with growing magnetic interaction strength the probability of forming self-assembled connections increases. As one can see for $\mu^2 = 5$, at large distances two linear SMPs undergo a closure transition by forming two independent rings. Also significant is the probability of finding a ring and an open chain configuration at large separation distances. As soon as the distance between the central particles of the two linear

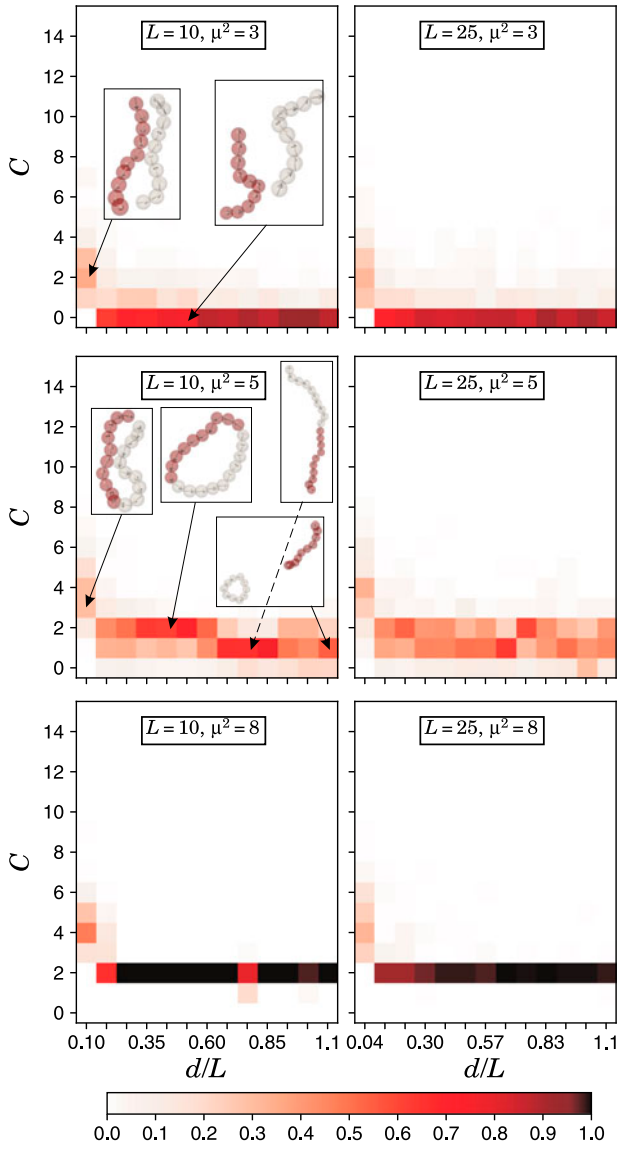

Figure 3. (Colour online) Probability distributions for two linear chain-like SMPs to form C self-assembled pair connections as a function of their relative characteristic separation, d/L. The values of μ^2 and SMP size are provided in the legend. Snapshots of some typical configurations are shown for $L = 10$. Snapshots for $L = 25$ are not provided for the sake of clarity due to their difficult visualisation. The colour scale indicates the probability of every value of C, ranging from white, for zero probability, to black for probability one.

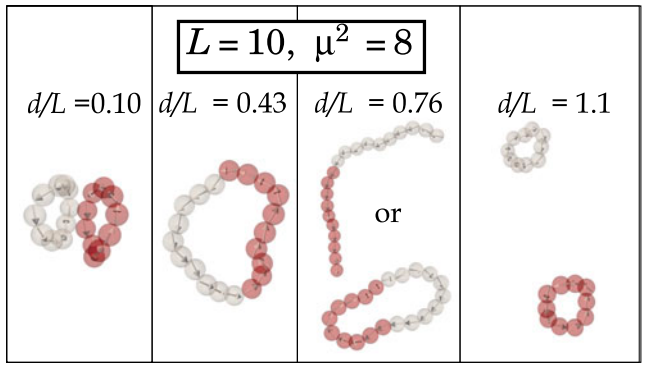

Figure 4. (Colour online) Typical structural motifs formed by linear SMPs with $L = 10$ and $\mu^2 = 8$ at a given relative separation d/L between the fixed central particles.

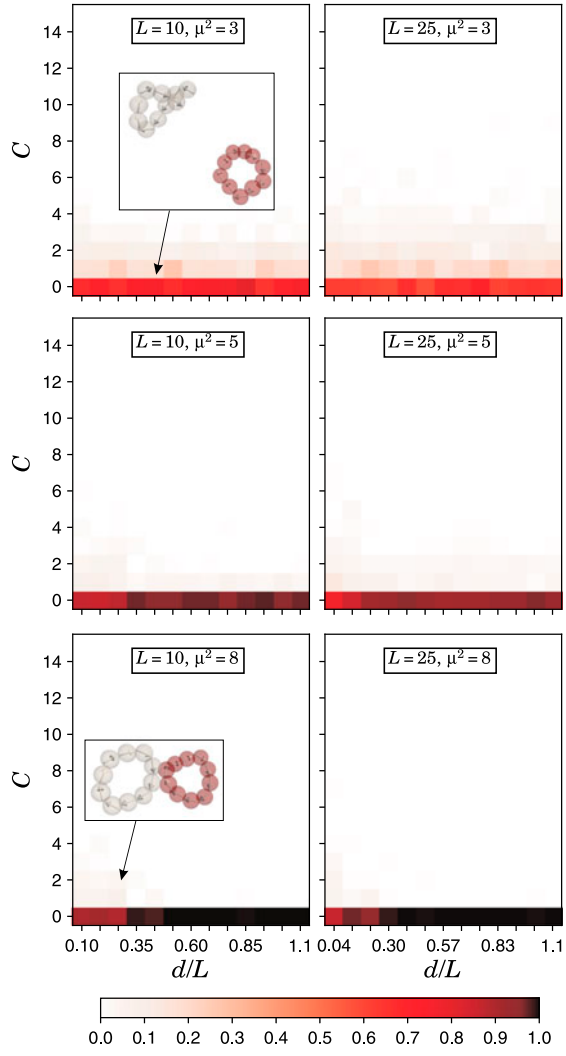

Figure 5. (Colour online) Probability distributions, indicated by a colour scale, for two ring SMPs to form C self-assembled connections as a function of their relative characteristic separation, d/L. The values of μ^2 and SMP size are provided in the legend.

SMPs becomes small enough for their ends to touch, the chains form a single ring, which then evolves into a double loop with decreasing d/L. By increasing further the value of μ^2, the probability of observing isolated open chains vanishes. Snapshots of the characteristic configurations observed for $\mu^2 = 8$ are provided separately in Figure 4 for the sake of clarity. From these results we can conclude that, for highly diluted systems, mainly open or closed loop structures of isolated SMPs would be observed for moderate to strong dipole–dipole interactions, with open structures being less probable as the latter become stronger. In general, it is reasonable to expect that the self-assembly in highly diluted systems of SMPs of any morphology will correspond mainly to internal rearrangements of the cross-linked backbone of individual clusters – typically, into closed loop structures – rather than the formation of aggregates of different SMPs. In contrast, for high concentrations of SMPs one can expect the inversion of this tendency, with the observation of a significant degree of external self-assembly – i.e. the self-

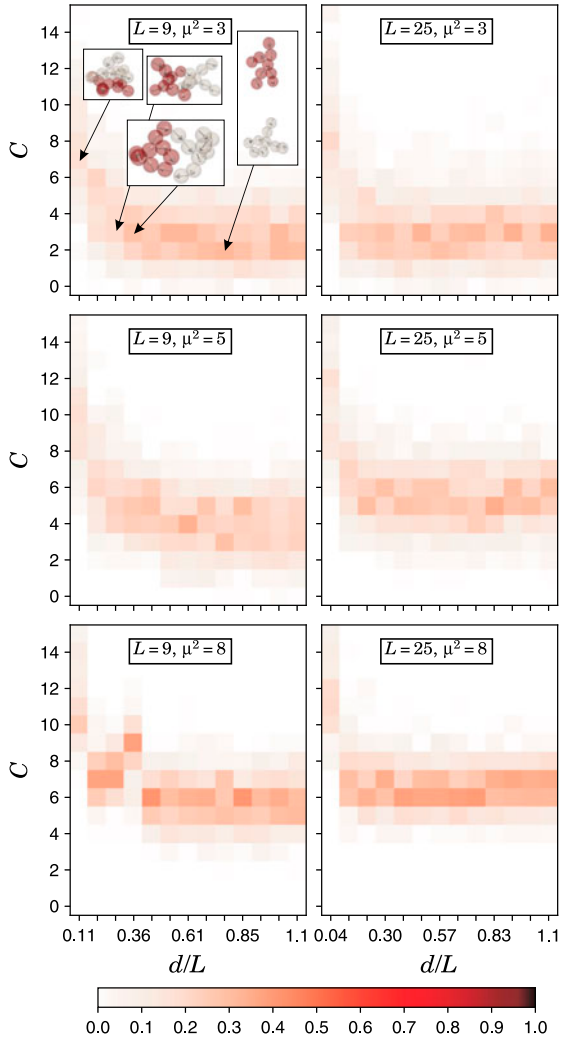

Figure 6. (Colour online) Probability distributions, indicated by a colour scale, for two X-junction SMPs to form C self-assembled connections as a function of their relative characteristic separation, d/L. The values of μ^2 and SMP size are provided in the legend.

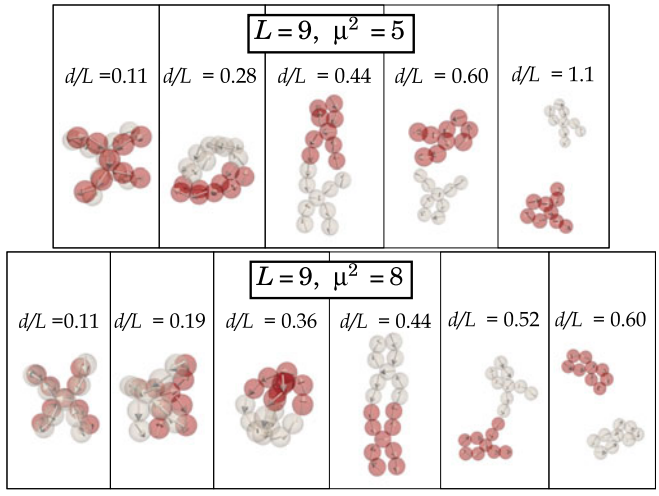

Figure 7. (Colour online) Typical structural motifs formed by two X-junction SMPs with size $L = 9$ and different relative characteristic separation distances, d/L, observed for $\mu^2 = 5$ (top row) and $\mu^2 = 8$ (bottom row).

assembly of different SMPs into larger aggregates – and the multi-loop topology as a dominant structural motif.

The next structure we analyse is the ring SMP. In Figure 5 one can see the probability distributions for two ring SMPs to form C self-assembled connections as a function of d/L. Due to the fact that nearly head-to-tail cross-linked dipolar particles keep, when arranged into rings or other closed structures, an almost zero net magnetic moment, makes the self-assembly of these SMPs essentially negligible. Here, this behaviour is observed for all sampled conditions. At this point, the comparison of linear and ring SMPs provides a first indication of what can be one of the main factors determining the different degrees of self-assembly corresponding to each topology: the amount of open chain ends.

The important role of the open chain ends in the self-assembly behaviour of the different SMPs is further emphasised by the results obtained for pairs of X-junction morphologies. These results are summarised in Figures 6 and 7. The probability distributions of C as a function of d/L, shown in Figure 6, indicate the existence of a richer variety of self-assembled structures, even at low μ^2. This is due to the fact that the X-junction morphology has, for example, twice as many open ends as the linear SMP. This increases the amount of different ways to form self-assembled motifs. In this regard, one can think of an analogy with chemical valency or with the self-assembly valency in patchy colloids [54,55]. In addition, a small SMP with X-junction shape is less likely to get their open ends involved in the formation of internal self-assembled structures – typically, as already mentioned above, closed loops – than linear chains or Y-junctions of similar size, keeping instead their free ends available for the self-assembly with other SMPs. The reason for this is related to the relatively shorter length of linear segments with open ends in the X-junction structure, which demands a higher local bending of the chain backbone in order to connect such open ends to other particles within the same SMP and form internal loops. Since the backbone has a finite intrinsic rigidity, led by the chain bonds and the dipole–dipole interactions [29,56], such bending can be unreachable for too small SMP sizes. Therefore, small X-junction morphologies are particularly favourable for external self-assembly. Figure 6 also shows how the probability to form energetically favourable connections increases with growing μ^2. In this case, the observation of the characteristic self-assembled structures, whose main examples are shown in Figure 7, is particularly interesting. The maximum separation distance at which external self-assembly can be observed is $d/L \sim 0.6$. At larger distances and with growing μ^2, the free ends within the same SMP tend to connect to each other in pairs, forming closed internal loops. For $\mu^2 = 8$, the most probable configuration is the resulting from the self-assembly of the four free ends into two pairs, forming a double loop structure. At intermediate distances, $0.3 \lesssim d/L \lesssim 0.6$, the external self-assembly of two pairs of free ends becomes dominant, so that the two SMPs form a large central closed loop, whereas the remaining free ends tend to form internal small loops. The most interesting structural motif is observed in a narrow separation region around $d/L \sim 0.28$ for $\mu^2 = 5$ and $d/L \sim 0.36$ for $\mu^2 = 8$: here, a cage-like structure is formed by means of the external self-assembly of the four pairs of free ends. This peculiar structure suggests its potential use as a

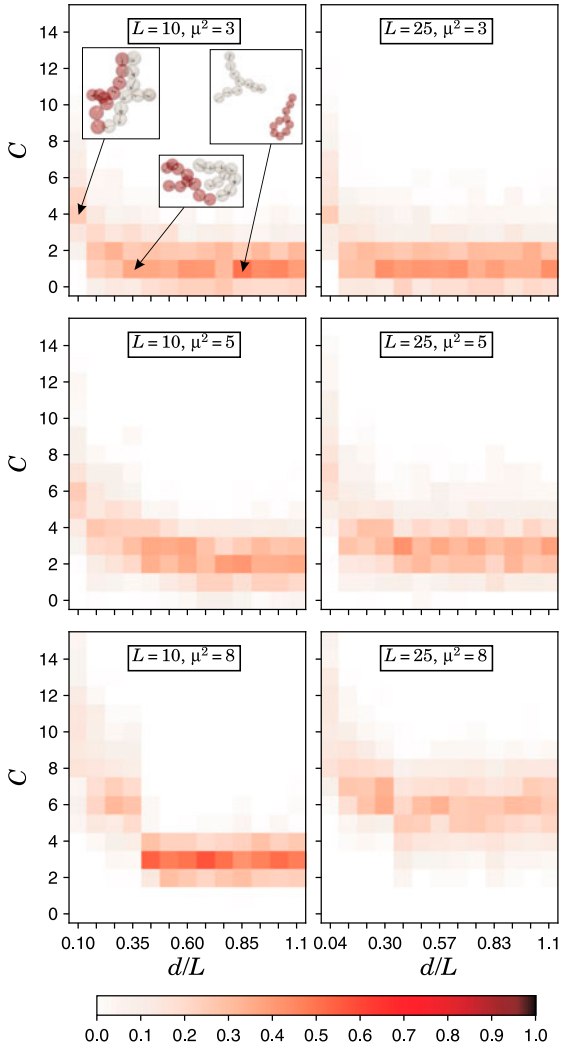

Figure 8. (Colour online) Probability distributions, indicated by a colour scale, for two SMPs of Y2-junction morphology to form C self-assembled connections as a function of their relative characteristic separation, d/L. The values of μ^2 and SMP size are provided in the legend. These results are also representative for the case of the Y1-junction morphology.

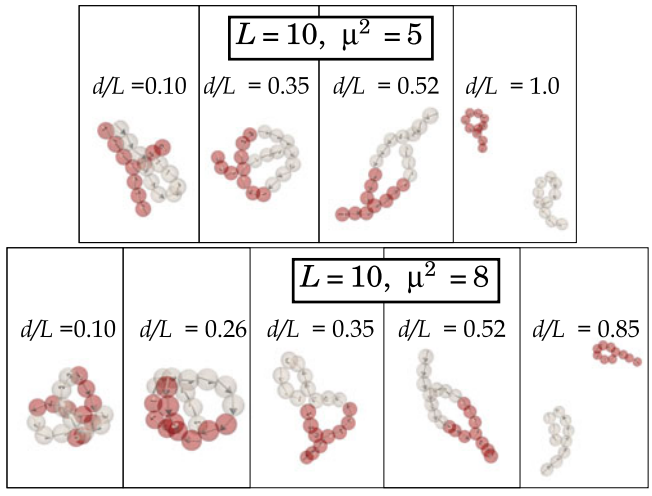

Figure 9. (Colour online) Examples of typical structural motifs formed by two Y2-junction SMPs with size $L = 10$ and different relative characteristic separation distances, d/L, observed for $\mu^2 = 5$ (top row) and $\mu^2 = 8$ (bottom row).

magnetically controllable container, able to enclose some small material by spontaneous self-assembly and release it when an external magnetic field, strong enough to disassemble the SMPs' aggregate, is applied. Finally, at shorter separation distances, there is a clear jump in the amount of connections led by the self-assembly of the two SMPs into a nearly flat, full contact structure with all dipoles arranged in antiparallel pairs.

Finally, we analyse the Y-junction morphologies. The first important observation is that, for the range of parameters sampled here, we found no significant differences in the probability distributions of self-assembled connections corresponding to Y1 and Y2 morphologies. It is also worth to underline that the grand canonical simulations mentioned above [40] show that the probabilities for free particles to form spontaneously Y-junctions of each type are identical. On the other hand, one can expect that the application of external fields will impose different orientations to each type of Y-junction, but to analyse the response of the different morphologies to external fields is beyond the scope of this work. Therefore, regarding the present discussion, we will consider the Y1 and Y2 morphologies as indistinguishable. Figures 8 and 9 correspond to the results obtained for the Y2 case. The probability distributions for the self-assembled connections, C, as a function of the relative separation, shown in Figure 8, display a behaviour similar to the observed for X-junctions, but with a slight shift towards lower values of this parameter. Roughly, one can see that the Y-junction is quantitatively in between the linear chain and the X-junction behaviours, further supporting the idea of the amount of free chain ends as one of the main factors in the self-assembly of these systems. For instance, except for very short separation distances, at $\mu^2 = 3$ we can see that C is distributed around a central value $\bar{C} \sim 1$, whereas for X-junctions we observed $\bar{C} \sim 2$ and for linear chains and rings $\bar{C} \sim 0$. Figure 9 shows examples of the different characteristic structures for $\mu^2 = 5$ and $\mu^2 = 8$. At large separation distances, Y-junction SMPs tend to form one closed internal ring, keeping one free chain end. At intermediate distances, the external self-assembly of two free ends from each SMP to form a large closed loop is also observed, whereas the remaining free end of each cluster is not involved in any self-ssembly. At shorter distances the self-assembled structures become more complex, with two pairs of free ends from each SMP still forming a closed loop but also involving the remaining free ends, which tend to connect to the central particle of the opposite SMP. This is favoured by the increase of μ^2 and the decreasing of d/L. The resulting structure is close to the cage-like aggregate observed for X-junctions, and its appearance is clearly signalled for $\mu^2 = 8$ by the shift of the C distribution at $d/L \sim 0.36$. Finally, at very close separation distances, the Y-junction SMPs can form full contact antiparallel structures or nearly flat multi-loop shapes.

4. Conclusions and outlook

In this work, we have undertaken a first step in the analysis of the self-assembly behaviour of SMPs, or SMPs, by performing computer simulations for different morphologies and selected values of the strength of their magnetic interactions. For their morphologies, we considered the typical basic structures observed in dispersions of free magnetic colloidal particles. For

simplicity, we focused on the behaviour a pair of identical small SMPs, mimicking the effect of the concentration by fixing the characteristic separation distance between them.

Our results predict that the amount of free chain ends of a given SMP morphology is determinant for the degree of self-assembly and the complexity of the resulting structures, playing a role that we can describe as a self-assembly 'valency'. Ring morphology – with no free chain ends, i.e. with zero self-assembly valency – is essentially inert, not participating in any self-assembly unless it is forced to interact with other aggregates by imposing a very close proximity. Linear chains – with valency 2 – tend to form simple closed rings or, for very high magnetic interactions and/or densities, multi-loops. Y-junction SMPs – with valency 3 – have a richer self-assembly behaviour, forming internal or external single rings at large separation distances and multi-loop, nearly cage-like structures at short separation distances. Finally, X-junction – that has valency 4 – is the morphology more prone to form self-assembled structures, including clear cage-like shapes at short separation distances.

In difference with the linear chain and ring structures, well-known in the context of dispersions of free magnetic particles, the cage-like structures observed for Y- and X-junction SMPs are, to our best knowledge, magnetically self-assembled morphologies never reported before. The cage-like structures formed by X-junction SMPs are particularly interesting for technological applications, as they can be conceived as magnetically actuated containers that can enclose and release small cargos. This observation points SMPs as promising building blocks of advanced magnetoresponsive microstructured materials. We hope this will encourage further research efforts on these systems.

Currently, we are planning to extend the present study by analysing non-homogeneous systems. By combining different SMP morphologies, we expect to find more novel self-assembled structures. The response to external fields of these systems will be also studied. Finally, an extension to larger systems, with actual dispersions of SMPs at different concentrations, will be also performed.

Acknowledgements

Computer simulations were performed at the Ural Federal University Computing Cluster.

Disclosure statement

No potential conflict of interest was reported by the authors.

Funding

This research has been supported by the Russian Science Foundation [grant number 17-72-10145]. J.J.C. and T.S. acknowledge funding from a grant awarded by the Conselleria d'Innovació, Recerca i Turisme del Govern de les Illes Balears and the European Social Fund (ESF). T.S. also acknowledges financial support from the Spanish Ministerio de Economía y Competitividad and the European Regional Development Fund, [Project number FIS20015-63628-C2-2-R] (AEI/FEDER, UE). P.A.S and S.S.K acknowledge support from the Austrian Research Fund (FWF) [START-Projekt Y 627-N27]. S.S.K. also acknowledges support from the European Commission ETN-COLLDENSE [H2020-MSCA-ITN-2014], [grant number 642774]. The authors would like to thank F. Sciortino for his valuable contribution to the GCMC simulation results.

ORCID

D. A. Rozhkov http://orcid.org/0000-0001-6724-8551
E. V. Novak http://orcid.org/0000-0002-4034-6861
P. A. Sánchez http://orcid.org/0000-0003-0841-6820
S. S. Kantorovich http://orcid.org/0000-0001-5700-7009

References

[1] Whitesides GM, Grzybowski B. Self-assembly at all scales. Science. 2002;295:2418–2421.
[2] Thiruvengadathan R, Korampally V, Ghosh A, et al. Nanomaterial processing using self-assembly-bottom-up chemical and biological approaches. Rep Prog Phys. 2013;76:066501.
[3] Stuart MAC, Huck WTS, Genzer J, et al. Emerging applications of stimuli-responsive polymer materials. Nat Mater. 2010;9:101–113.
[4] Singamaneni S, Bliznyuk VN, Binek C, et al. Magnetic nanoparticles: recent advances in synthesis, self-assembly and applications. J Mater Chem. 2011;21:16819–16845.
[5] Colombo M, Carregal-Romero S, Casula MF, et al. Biological applications of magnetic nanoparticles. Chem Soc Rev. 2012;41:4306–4334.
[6] Vékás L, Avdeev M, Bica D. Magnetic nanofluids: synthesis and structure. In: Shi D, editor. Nanoscience in biomedicine. Springer: Berlin Heidelberg; 2009. p. 650–728.
[7] Odenbach S, editor. Colloidal magnetic fluids. Vol. 763 of Lecture notes in physics, Berlin: Springer-Verlag; 2009.
[8] Park BJ, Fang FF, Choi HJ. Magnetorheology: materials and application. Soft Matter. 2010;6:5246–5253.
[9] Torres-Diaz I, Rinaldi C. Recent progress in ferrofluids research: novel applications of magnetically controllable and tunable fluids. Soft Matter. 2014;10:8584–8602.
[10] Klokkenburg M, Vonk C, Claesson EM, et al. Direct imaging of zero-field dipolar structures in colloidal dispersions of synthetic magnetite. J Am Chem Soc. 2004;126:16706–16707.
[11] Klokkenburg M, Dullens RPA, Kegel WK, et al. Quantitative real-space analysis of self-assembled structures of magnetic dipolar colloids. Phys Rev Lett. 2006;96:037203.
[12] Furst EM, Gast AP. Micromechanics of dipolar chains using optical tweezers. Phys Rev Lett. 1999 May;82:4130–4133.
[13] Kantorovich S, Ivanov AO, Rovigatti L, et al. Nonmonotonic magnetic susceptibility of dipolar hard-spheres at low temperature and density. Phys Rev Lett. 2013;110:148306.
[14] Kantorovich SS, Ivanov AO, Rovigatti L, et al. Temperature-induced structural transitions in self-assembling magnetic nanocolloids. Phys Chem Chem Phys. 2015;17:16601–16608.
[15] Zrínyi M. Intelligent polymer gels controlled by magnetic fields. Colloid Polym Sci. 2000;278:98–103.
[16] Thévenot J, Oliveira H, Sandre O, et al. Magnetic responsive polymer composite materials. Chem Soc Rev. 2013;42:7099–7116.
[17] Odenbach S. Microstructure and rheology of magnetic hybrid materials. Arch Appl Mech. 2016;86:269–279.
[18] Goubault C, Jop P, Fermigier M, et al. Flexible magnetic filaments as micromechanical sensors. Phys Rev Lett. 2003;91:260802.
[19] Dreyfus R, Baudry J, Roper ML, et al. Microscopic artificial swimmers. Nature. 2005;437:862–865.
[20] Ērglis K, Zhulenkovs D, Sharipo A, et al. Elastic properties of dna linked flexible magnetic filaments. J Phys-Condens Mat. 2008;20:204107.
[21] Benkoski JJ, Breidenich JL, Uy OM, et al. Dipolar organization and magnetic actuation of flagella-like nanoparticle assemblies. J Mater Chem. 2011;21:7314–7325.
[22] Hill LJ, Pyun J. Colloidal polymers via dipolar assembly of magnetic nanoparticle monomers. ACS Appl Mater Interfaces. 2014;6:6022–6032.
[23] Corr SA, Byrne SJ, Tekoriute R, et al. Linear assemblies of magnetic nanoparticles as mri contrast agents. J Am Chem Soc. 2008;130:4214–4215.
[24] Wang H, Yu Y, Sun Y, et al. Magnetic nanochains: a review. Nano. 2011;06:1–17.

[25] Tokarev A, Gu Y, Zakharchenko A, et al. Reconfigurable anisotropic coatings via magnetic field-directed assembly and translocation of locking magnetic chains. Adv Funct Mater. 2014;24:4738–4745.
[26] Sánchez PA, Pyanzina ES, Novak EV, et al. Supramolecular magnetic brushes: the impact of dipolar interactions on the equilibrium structure. Macromolecules. 2015;48:7658–669.
[27] Sánchez PA, Pyanzina ES, Novak EV, et al. Magnetic filament brushes: tuning the properties of a magnetoresponsive supramolecular coating. Faraday Discuss. 2016;186:241–263.
[28] Pyanzina ES, Sánchez PA, Cerdà JJ, et al. Scattering properties and internal structure of magnetic filament brushes. Soft Matter. 2017;13:2590–2602.
[29] Sánchez PA, Cerdà JJ, Sintes T, et al. The effect of links on the interparticle dipolar correlations in supramolecular magnetic filaments. Soft Matter. 2015;11:2963–2972.
[30] Biswal SL, Gast AP. Mechanics of semiflexible chains formed by poly(ethylene glycol)-linked paramagnetic particles. Phys Rev E. 2003 Aug;68:021402.
[31] Byrom J, Han P, Savory M, et al. Directing assembly of DNA-coated colloids with magnetic fields to generate rigid, semiflexible, and flexible chains. Langmuir. 2014;30:9045–9052.
[32] Srivastava S, Nykypanchuk D, Fukuto M, et al. Two-dimensional dna-programmable assembly of nanoparticles at liquid interfaces. J Am Chem Soc. 2014;136:8323–8332.
[33] Tian Y, Wang T, Liu W, et al. Prescribed nanoparticle cluster architectures and low-dimensional arrays built using octahedral dna origami frames. Nat Nano. 2015;10:637–644.
[34] Byrne SJ, Corr SA, Gun'ko YK, et al. Magnetic nanoparticle assemblies on denatured dna show unusual magnetic relaxivity and potential applications for MRI. Chem Commun. 2004;2560–2561.
[35] Sarkar D, Mandal M. Static and dynamic magnetic characterization of DNA-templated chain-like magnetite nanoparticles. J Phys Chem C. 2012;116:3227–3234.
[36] Cerdà JJ, Sánchez PA, Sintes T, et al. Phase diagram for a single flexible Stockmayer polymer at zero field. Soft Matter. 2013;9:7185–7195.
[37] Cerdà JJ, Sánchez PA, Lüsebrink D, et al. Flexible magnetic filaments under the influence of external magnetic fields in the limit of infinite dilution. Phys Chem Chem Phys. 2016;18:12616–12625.
[38] Wei J, Song F, Dobnikar J. Assembly of superparamagnetic filaments in external field. Langmuir. 2016;32:9321–9328.
[39] Novak E, Rozhkov D, Sánchez P, et al. Self-assembly of designed supramolecular magnetic filaments of different shapes. J Magn Magn Mater. 2017;431:152–156.
[40] Ronti M, Rovigatti L, Tavares JM, et al. Accurate free energy calculations for rings and chains formed by dipolar hard spheres. Soft Matter. 2017. submitted.
[41] Weeber R, Kantorovich S, Holm C. Deformation mechanisms in 2d magnetic gels studied by computer simulations. Soft Matter. 2012;8:9923–9932.
[42] Annunziata MA, Menzel AM, Löwen H. Hardening transition in a one-dimensional model for ferrogels. J Chem Phys. 2013;138:204906.
[43] Tarama M, Cremer P, Borin DY, et al. Tunable dynamic response of magnetic gels: impact of structural properties and magnetic fields. Phys Rev E. 2014;90:042311.
[44] Weeber R, Kantorovich S, Holm C. Ferrogels cross-linked by magnetic particles: field-driven deformation and elasticity studied using computer simulations. J Chem Phys. 2015;143:154901.
[45] Pessot G, Weeber R, Holm C, et al. Towards a scale-bridging description of ferrogels and magnetic elastomers. J Phys: Condens Matter. 2015;27:325105.
[46] Pessot G, Löwen H, Menzel AM. Dynamic elastic moduli in magnetic gels: normal modes and linear response. J Chem Phys. 2016;145:104904.
[47] Weeks JD, Chandler D, Andersen HC. Role of repulsive forces in determining the equilibrium structure of simple liquids. J Chem Phys. 1971;54:5237–5247.
[48] Allen MP, Tildesley DJ. Computer simulation of liquids. 1st ed. Oxford Science Publications; Oxford: Clarendon Press; 1987.
[49] Frenkel D, Smit B. Understanding molecular simulation. Academic Press; 2002.
[50] Cerdà JJ, Kantorovich S, Holm C. Aggregate formation in ferrofluid monolayers: simulations and theory. J Phys-Condens Mat. 2008;20:204125.
[51] Kantorovich S, Cerdà JJ, Holm C. Microstructure analyisis of monodisperse ferrofluid monolayers: theory and simulation. Phys Chem Chem Phys. 2008;10:1883–1895.
[52] Limbach HJ, Arnold A, Mann BA, et al. ESPResSo - an extensible simulation package for research on soft matter systems. Comput Phys Commun. 2006;174:704–727.
[53] Arnold A, Lenz O, Kesselheim S, et al. Espresso 3.1: Molecular dynamics software for coarse-grained models. In: Griebel M, Schweitzer MA, editors., Meshfree methods for partial differential equations vi, Vol. 763 of Lecture notes in computational science and engineering Springer: Berlin; 2013. p. 1–23.
[54] Tartaglia P, Sciortino F. Association of limited valence patchy particles in two dimensions. J Phys: Condens Matter. 2010;22:104108.
[55] Smallenburg F, Sciortino F. Liquids more stable than crystals in particles with limited valence and flexible bonds. Nat Phys. 2013;9:554–558.
[56] Sánchez PA, Cerdà JJ, Sintes T, et al. Effects of the dipolar interaction on the equilibrium morphologies of a single supramolecular magnetic filament in bulk. J Chem Phys. 2013;139:044904.